LABORATORY TESTS ON GEOTEXTILE REINFORCED DUNE SAND

Talal Obeid Al-Refeai*

Department of Civil Engineering
King Saud University
Riyadh, Saudi Arabia

الخلاصـــة :

تَـمَّ إجرا عدد من اختبارات الضغط الثلاثي المحاور للتوصل الى معرفة صفات (الإجهاد ـ الانفعال) للرمل الـمُـقـوّىٰ بالنسيج ، وكذلك لملاحظة أثر تعديل خواص مختلفة للنسيج وللتربة المستخدمة على التغيير العنصري للتربة من جراء استخدام النسيج الـمُقـوّىٰ ، كما جرى إعداد اختبارات الضغط الأحادي المحور على قوالب من عـيّنات الرمل لمعاينة تأثير النسيج الخارجي الـمُـقـوّىٰ لعـيّنات التربة على عناصرها الحبيبية الـمُـقـوّاة من الداخل .

وتُـبـيِّـن النتائج المستوفاة حصول زيادة ملحوظة في قدرة التحمل الـقُـصوى والانفعال المحوري عند الانهيار ، والحد من نقص مقاومة القص لما بعد الذروة للتربة الرملية المقواة بنسيج داخلي ، كما ظهر نقص في معدل صلابة الرمل الـمُـقـوّىٰ عند درجات انفعال منخفضة جدا (اقل من ١٪) ، حيث لوحظ زيادة تأثير هذا النقص عند زيادة عدد طبقات وصلابة النسيج الداخلي . وإنَّ زيادة نسبة (المسافة البَـيْـنِـيَّـة إلى القطر) لأكثر من (واحد) لم يكن لها تأثير يذكر على قوة تحـمّـل الرمل الـمُقـوّىٰ .

وبالاضافة الى ذلك فان استخدام النسيج الـمُـقـوّىٰ الداخلي يزيد قوة احتمال الضغط الـقُـصوى للرمل الـمُـغـلَّف بالنسيج . لذا فإن الصلابة الكلـيَّـة للرمل المغلف بالنسيج الـمُـقـوّىٰ يمكن التأثير عليها إلى حـدٍّ بعيد بواسطة معامل صلابة النسيج الـمُـقـوّىٰ الخارجي وكذلك بعدد طبقات ومعامل النسيج الـمُـقـوّىٰ الداخلي .

*Address for correspondence:
Department of Civil Engineering
King Saud University
P.O. Box 800, Riyadh 11421
Saudi Arabia

ABSTRACT

Laboratory triaxial compression tests were performed to determine the stress–Strain response of sand reinforced with fabric, and to observe the influence of various inclusion properties and soil properties on the constitutive behavior of fabric reinforced sand. Uniaxial compression tests were also run on encapsulated sand specimens to examine the effect of external fabric encapsulation on constitutive behavior of internally reinforced granular materials.

Fabric inclusions markedly increased the ultimate strength, increased the axial strain at failure, and caused limited reductions in post-peak shearing resistance. At very low strain (<1%) fabric reinforcement produced a loss of stiffness with the effect being more pronounced the greater the number of layers and the stiffer the reinforcement. Reinforcements placed at a spacing:diameter ratio of more than one had little effect on strength.

Fabric inclusions increased the ultimate compressive strength of encapsulated sand. The overall stiffness of an encapsulated/internally reinforced sand can be controlled to a large extent by the modulus of the encapsulating fabric, and the number of layers and modulus of internal reinforcing fabric.

LABORATORY TESTS ON GEOTEXTILE REINFORCED DUNE SAND

INTRODUCTION

Synthetic engineering fabrics or "geotextiles" have become increasingly important in civil engineering applications in recent years. The main applications include drainage, erosion control, separation, and reinforcement; over 200 specific uses have been identified within these general application areas [1–3]. An experimental investigation has been undertaken to define the role and influence of fabric properties (fabrication and/or material characteristics) on the structural reinforcement of sand. Triaxial tests on samples of sand reinforced with disks of fabric were conducted for this purpose. Uniaxial compression tests were also run on encapsulated sand specimens to study the effect of external fabric encapsulation on the constitutive behavior of internally reinforced granular material.

EARTH REINFORCEMENT THEORIES

There are different concepts to explain the mechanics of earth reinforcement with oriented inclusion layers [4–7]. Mitchell and Schlosser [8] and Ingold [9] described and compared in full detail these concepts. The two most significant concepts are described briefly below.

The Enhanced Confining Pressure Concept

Yang [6] conducted triaxial tests on sand specimens reinforced by horizontal layers of fiberglass nets. He assumed that the sand failed at a constant effective stress ratio

$$\left(\frac{\sigma_3}{\sigma_1}\right)_f = \tan^2\left(45 - \frac{\phi_s}{2}\right). \tag{1}$$

Yang concluded that any increase in σ_{1f} at failure of a reinforced specimen was due to an equivalent confining stress increase $\Delta\sigma_3$. Yang hypothesized that tensile restraint in the reinforcement induced this equivalent confining stress increase, $\Delta\sigma_3$. From the known Mohr–Coulomb Formulation for the strength of a cohesionless material it follows that

$$\sigma_{1f} = \sigma_{3f} N_\phi = (\sigma_3 + \Delta\sigma_3) N_\phi , \tag{2}$$

where:

σ_{1f} = maximum major principal stress of reinforced triaxial specimen;
σ_{3f} = equivalent minor principal stress for reinforced triaxial specimen;
σ_3 = initial confining pressure;
$\Delta\sigma_3$ = equivalent minor principal stress increase for reinforced triaxial specimen; and
N_ϕ = $\tan^2(45+\phi_s/2)$; where ϕ_s = angle of internal friction of unreinforced sand.

The Anisotropic or Pseudo-Cohesion Concept

Schlosser and Long [5] tested sand specimens reinforced by aluminum foil disks. Schlosser and Long proposed that reinforcements induced an anisotropic or pseudo-cohesion (C_R) which was a function of their spacing and tensile strength. They defined the strength of the reinforced sand by

$$\sigma_{1f} = \sigma_3 N_\phi + 2C_R \sqrt{N_\phi}. \tag{3}$$

The additional strength $\Delta\sigma_1$ in excess of the frictional strength of unreinforced specimen was interpreted as being the effect of a pseudo-cohesion developed in the new composite material. The anisotropic or pseudo-cohesion (C_R) was computed from a force equilibrium analysis of a reinforced composite:

$$C_R = \frac{R_T}{\Delta H}\,\frac{\sqrt{N_\phi}}{2}, \tag{4}$$

where:

R_T = force per unit width of reinforcement at failure, and
ΔH = spacing between reinforcement layers.

Comparing Equations (2) and (3) with (4) indicates a direct correspondence between Yang's $\Delta\sigma_3$ and the Schlosser and Long $\Delta\sigma_1$ or C_R. Equations (2) and (3) yield:

$$\Delta\sigma_3 N_\phi = 2C_R \sqrt{N_\phi} \quad \text{or}$$

$$C_R = \Delta\sigma_3\,\frac{\sqrt{N_\phi}}{2}. \tag{5}$$

Equations (4) and (5) yield

$$\Delta\sigma_3 = \frac{R_T}{\Delta H}. \tag{6}$$

Thus, either the $\Delta\sigma_3$ or the C_R approach could be used equally well for analyzing the behavior of reinforced earth with continuous, oriented fabric layers for maximum strength conditions, where failure occurs by breaking of the reinforcement rather than pullout.

EXPERIMENTAL

Materials

Sand

A clean dune sand was used in this study. Typical properties of the sand are listed in Table 1.

Table 1. Properties of Dune Sand.

D_{10}	0.28 mm
D_{50}	0.41 mm
C_u	1.50
G_s	2.65
e_{max}	0.78
e_{min}	0.50
$(\phi_s)_{triaxial}$	39° (D_r = 86%)
	32° (D_r = 21%)

Fabric

Five geotextiles, each with different fabrication and/or material characteristics were employed in this study. These fabrics are described in Tables 2 and 3.

Triaxial Tests

A standard Geonor triaxial apparatus was used for testing fabric reinforced sand. All tests were carried out on cylindrical samples with a diameter of 36 mm and a height of 80 mm. The reinforcement consisted of circular disks of fabric which were cut from fabric sheets by rotating a heated sharpened aluminum tube (35 mm I.D.) on fabric placed over a wood block.

Table 2. Physical Properties of Geotextiles.

Fabric	Manufacturer	Filament	Fabrication Process	Nominal Thickness[a] (mm)	Mass per Unit Area[b] ($g\,m^{-2}$)
Geolon 400	Nicolon	Polypropylene multifilament	Woven	0.74	220
Geolon 200	Nicolon	Polypropylene tape	Woven	0.46	136
Typar 3601	Dupont	Polypropylene multifilament	Nonwoven heatbound	0.46	203
Typar 3401	Dupont	Polypropylene multifilament	Nonwoven heatbound	0.38	136
Fiberglass 196	Baymills	Glass yarns monofilament	Woven	1.09	1153

[a]ASTM D1777, [b]ASTM D1910/D 3776-85

Table 3. Mechanical Properties of Geotextiles.

Fabric	Tensile Strength (Grab Test) N	Elongation at Break %	Mullen Burst kPa	Secant Modulus[a] $kN\,m^{-1}$ at 5% Elongation
Geolon 400	1668×1108	30×18	2942	114×114
Geolon 200	892×892	20×20	2550	78×78
Typar 3601	922	63	1863	210
Typar 3401	598	62	1373	80
Fiberglass 196	–	8×10	–	471×192

[a]150×300 mm strip and 1% min^{-1} strain rate for woven fabrics.

Two different methods of constructing the samples were adopted, resulting in a dense and a loose deposit respectively. A dense ($e = 0.54$) packing of the sand was obtained using an "air pluviation" method. A constant pluviation height of about 400 mm was used to prepare all the specimens.

In order to obtain the maximum porosity or loosest packing, sand was placed in a tube (27 mm I.D.) inside the mold. The inner tube was then very carefully withdrawn from the mold leaving a loose deposit of sand behind. The void ratio of sample prepared in this manner was equal to 0.72.

For reinforced sand samples, the amount of dry sand required between consecutive layers of reinforcement was calculated in advance. Specimens were built up layer by layer. The predetermined amount of sand was deposited in the mold using one of the methods of deposition just described. The surface of the sand layer was leveled each time using a fine brush. The reinforcement disk was then placed on top and the process repeated until the desired number of reinforcement layers were inserted in the sample. The warp direction of the reinforcement was oriented in the same direction each time to minimize possible scattering of the results.

The number of reinforcement layers varied from 1 to 6. In any given test, the spacing between adjacent reinforcement layers was uniform and was twice the distance between the end of the specimen and the first layer as shown in Figure 1. The total height of the reinforced specimens was kept constant at 80 mm. The triaxial specimens were loaded to failure under five different confining pressures (49, 98, 196, 294, and 392 kPa) respectively.

Quasi-Uniaxial Compression Tests

Quasi-uniaxial compression tests were run on 140 mm high, 61 mm diameter specimens of dry dune sand encapsulated in two types of woven fabric sleeves, namely Geolon 400 and Geolon 200. All tests were run using a Tinius Olsen Testing Machine (53 kN maximum capacity).

Fabric manufacturers were unable to provide a unitary, woven, sleeve of 61 mm diameter. Accordingly, it was necessary to fabricate our own sleeves for testing purposes. In an effort to find an "efficient" way to bound fabrics together, several fastening or seaming method were tried, including adhesive glueing and manual sewing. Adhesive glueing did not work well because it either produced a very stiff seam which affected the vertical stiffness of the sleeve or a weak seam which tended to localize failure at the seam.

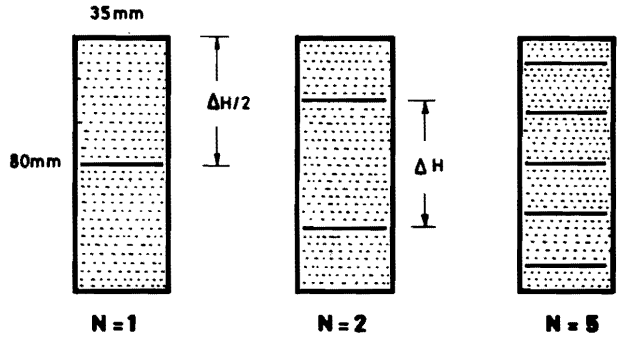

Figure 1. Fabric Position in Triaxial Test Specimens.

A sewn overlap seam 25 mm wide using a stiff polyester thread (90 N strength) was adopted to fabricate the sleeves. Interanal reinforcement in the shape of disks (59 mm in diameter) were used. The same methods used for preparing the fabric reinforced triaxial test specimens were also employed for preparing the sleeve samples.

Figure 2 shows a typical deformation pattern of dry, dense sand encapsulated in Geolon 200 and internally reinforced with 4 layers of Typar 3601 near failure.

TEST RESULTS AND DISCUSSION

Triaxial Tests

The Effect of Confining Pressure on the Strength of Reinforced Sand

Figure 3 shows the relationship between the confining pressure (σ_3) and the value at failure of the stress normal to reinforcement (σ_{1f}). Failure in a reinforced sand tends to occur by slippage at confining stress lower than a critical value and by excessive yielding or rupture of reinforcement at confining stress higher than a critical value. The break in $\sigma_1 - \sigma_3$ curves correspond to the critical confining stress in question. This behavior corroborates earlier triaxial test results reported by Yang [6] for fiberglass nets, Schlosser and Long [5] for aluminum foil, and Gray and others [10] for nonwoven fabric. A confining pressure equal to or exceeding 196 kPa was used in all subsequent tests in order to prevent slippage or pull out failures. It is also observed from

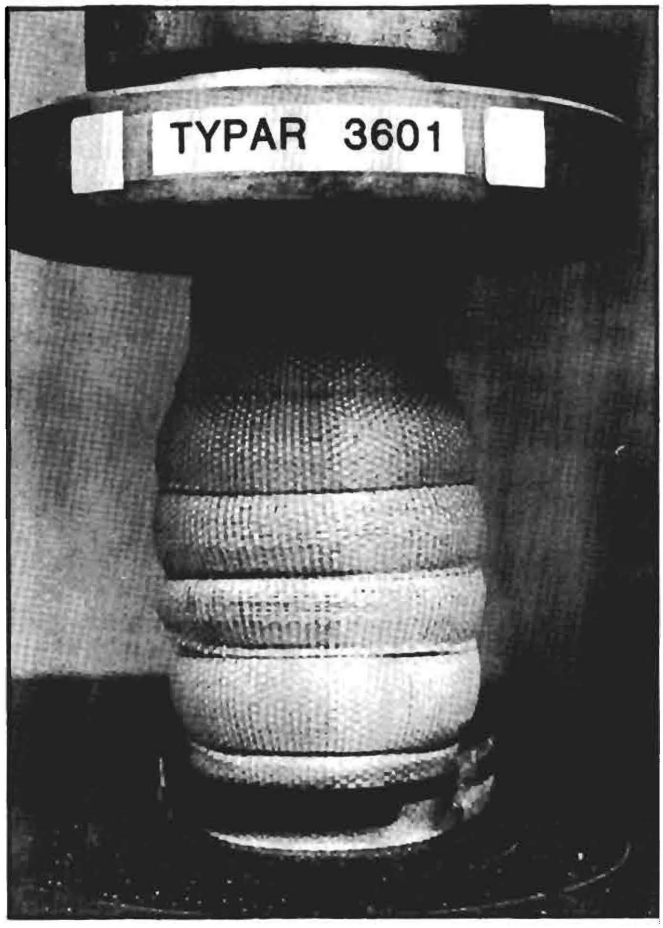

Figure 2. Deformed Shape of Encapsulated/Internally Reinforced Sand Tests in Uniaxial Compression.

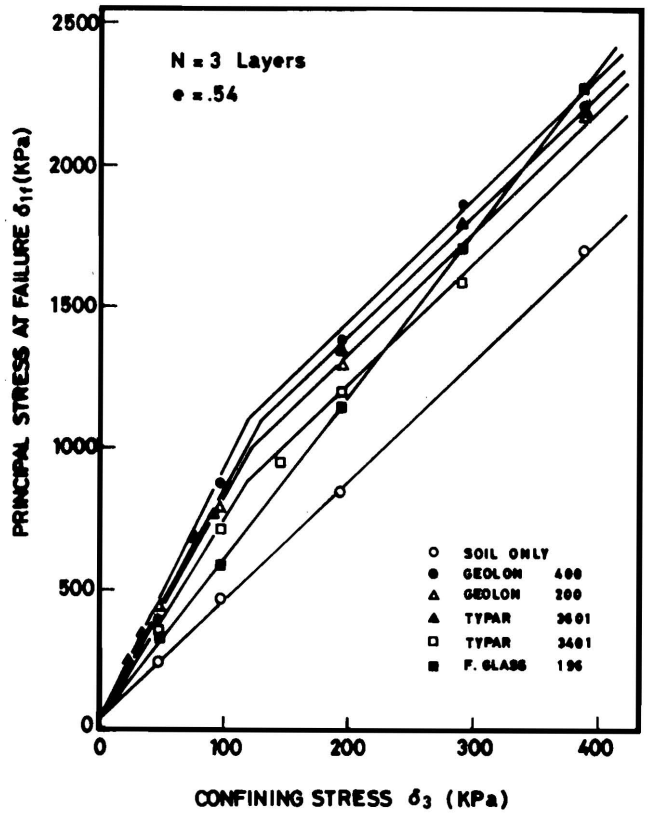

Figure 3. $\sigma_1-\sigma_3$ Curves from Triaxial Compression Tests on Dry, Dense Fabric Reinforced Sand.

Figure 3 that, above the critical confining stress, $\sigma_1-\sigma_3$ curves all tended to parallel the envelope for the unreinforced sand. These results indicate that the friction angle of sand was unaffected by the presence of the reinforcement. Also due to the smooth and slippery texture of the fiberglass fabric, failure of fiberglass reinforced sand was caused by sand particles sliding on the contact face and the critical confining stress was not reached. This is one of the reasons that fiberglass fabric was not used for further testing.

Influence of Amount of Reinforcement on Shear Strength of Reinforced Sand

Stress–strain relationships for fabric reinforced and unreinforced sand are shown in Figure 4. Fabric inclusion markedly increased the maximum principal stress difference ($\sigma_1-\sigma_3$) and limited reduction in post-peak shearing resistance. Increasing the number of layers caused a progressive increase in the peak strength.

It is interesting to note the relative efficiency of different types of reinforcement; Geolon 200 and Typar 3401 have the same modulus (E @ 5% = 80 kN m^{-1}) but Geolon 200 led to higher shear resistance as shown in Figure 4. This behavior can be explained as follows; the woven fabric (Geolon 200) exhibited a slightly larger interface friction than the nonwoven fabric (Typar 3401). In the case of woven fabric, the soil grains are free to penetrate into the openings in the fabric and there is actual physical interlocking between grains on opposite sides of the fabric, whereas in the case of melt bonded nonwoven fabric the soil grains cannot penetrate the fabric easily and hence the frictional resistance in this case is due to grain sliding onto the fabric surface. Using 3 layers of Typar 3401 also resulted in higher shear strength increases than those produced by 5 layers of the stiffer Typar 3601 (E @ 5% = 210 kN m^{-1}) up to strain at 2%.

Yang [6] presented a semi-empirical equation which relates the equivalent confining stress increase ($\Delta\sigma_3$) with the number of layers of reinforcement and the mechanical properties of the sand:

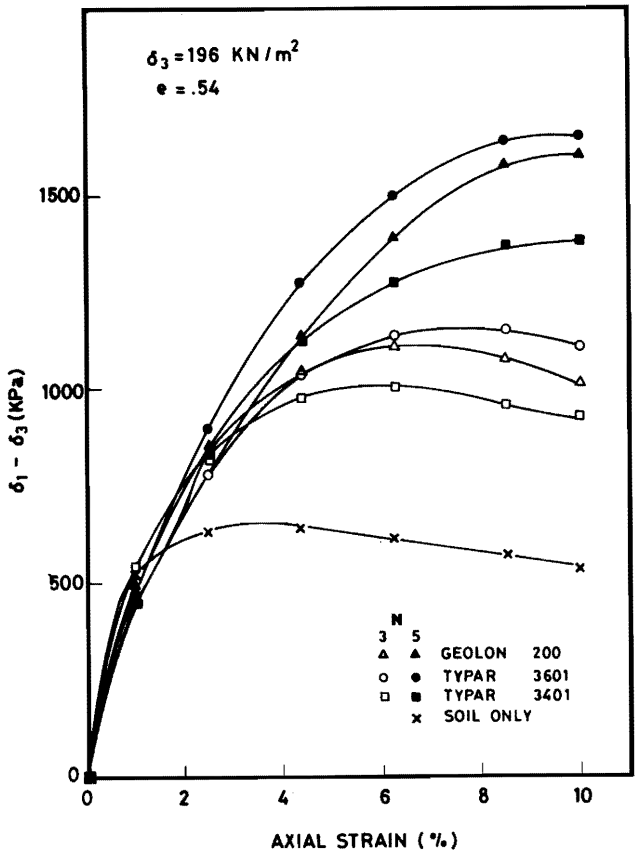

Figure 4. Stress–Deformation Relationships for Sand Reinforced with Different Layers of Various Fabric Reinforcement in Triaxial Compression.

$$\frac{\sigma_3 + \Delta\sigma_3}{\sigma_3} = \frac{1}{1 - G\,N_\phi \left(\frac{1}{2}\,\frac{d}{\Delta H}\right)^M}, \qquad (7)$$

where

σ_3 = initial confining pressure,
$\Delta\sigma_3$ = equivalent minor principal stress increase of reinforced triaxial specimen,
G, M = empirical constants,
N_ϕ = $\tan^2(45+\phi_s/2)$, where ϕ_s = angle of internal friction of unreinforced sand,
d = triaxial specimen diameter,
ΔH = spacing between reinforcement layers.

Two points of $d/\Delta H$ were selected for each fabric ($N = 3$ and 4) to determine the constants G and M. Figure 5 shows the curves predicted by Equation (7) and the experimental results of the triaxial test. The experimental results and the theoretical curve compare well. If average values from all tests of constant G and M were used in Equation (7), a better comparison between these two curves would

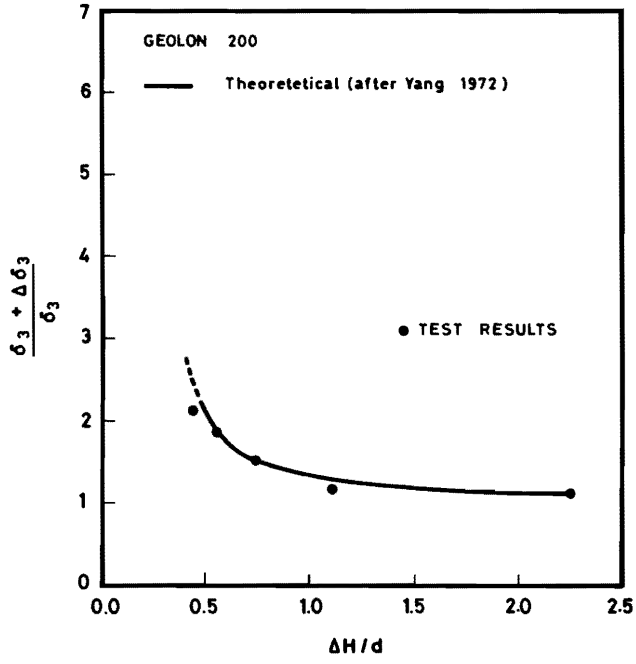

Figure 5. Relationship Between Spacing/Diameter Ratio and Strength Ratio for Fabric Reinforced Sand (Geolon 200).

have been observed. Figure 5 shows that reinforcements placed at spacing diameter ratios ($\Delta H/d$) more than one have little effect.

Figure 6 shows the relationships between the principal stress at failure (σ_{1f}) *versus* number of layers which indicates that strength increase is proportional to amount of reinforcement up to some limiting amount. Thereafter, the strength increase approaches an asymptotic upper limit.

Figure 7 presents the relation of the ratio of secant modulus of reinforced to unreinforced sand. The figure shows that the secant modulus varies significantly with both the strain and the number of layers. As the number of layers increases the secant modulus ratio tends to increase very rapidly. However, this increase was only observed at strain which exceed some threshold level — usually around 0.5 to 1 percent. At very low strains (<0.5%) reinforcement produced a loss of stiffness. This effect is more pronounced the greater the number of layers of reinforcement, the denser the soil and stiffer the reinforcement, as shown in Figure 8. These results can probably be explained by the fact that the reinforcement must be strained by the sand before it can have any influence. The reinforcement has a negligible effect on the response of the sand between the start of the test and an initial stage, simply because the

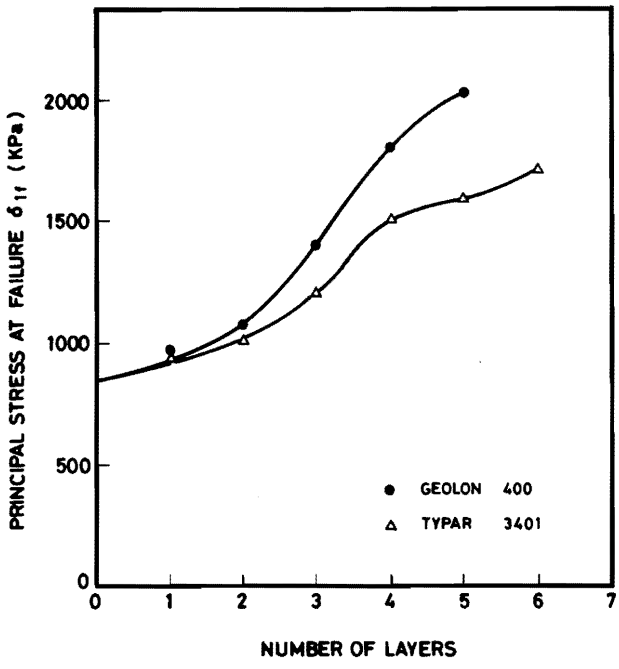

Figure 6. Principal Stress at Failure versus *Number of Layers for Fabric Reinforced Sand.*

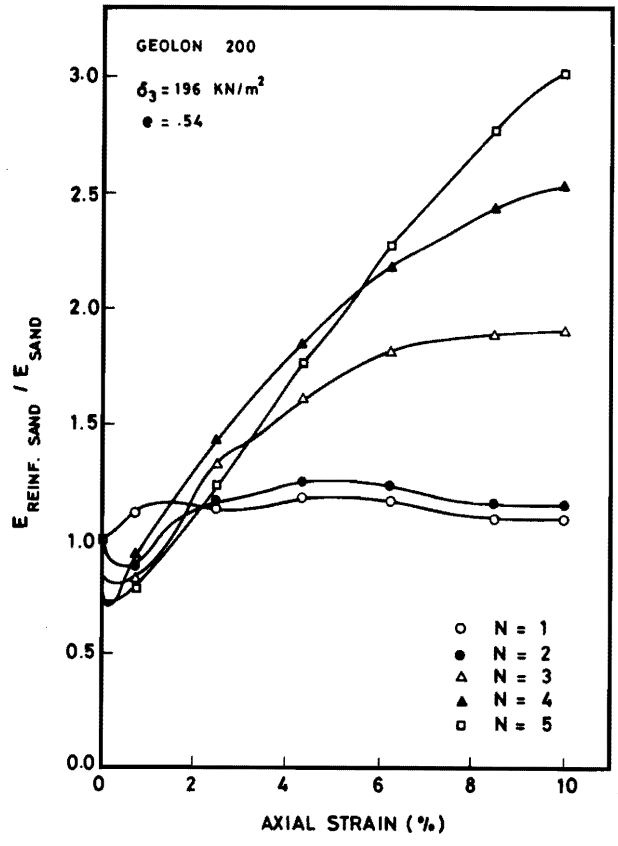

Figure 7. $E_{REINFORCED\ SAND}/E_{SAND}$ versus *Axial Strain in Triaxial Compression for Fabric Reinforced Sand (Geolon 200).*

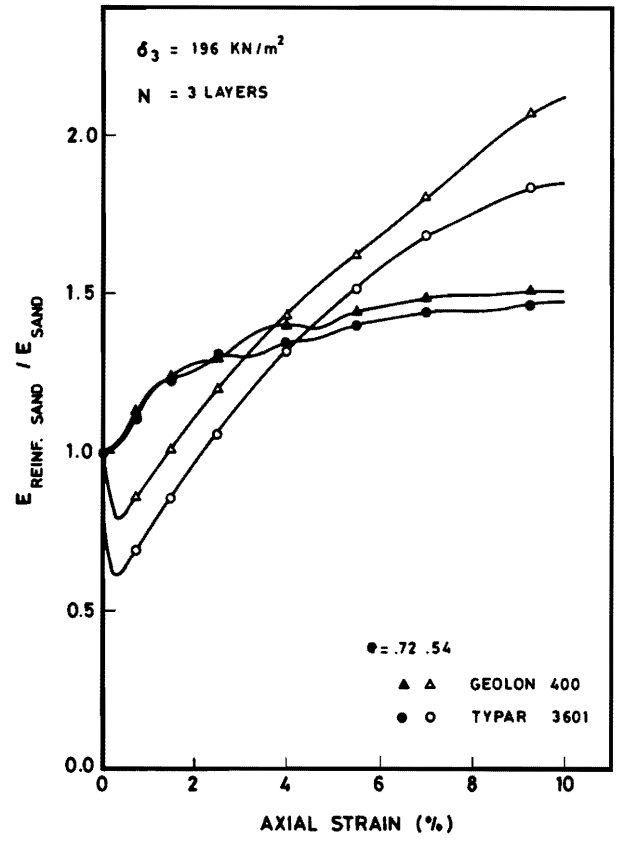

Figure 8. $E_{REINFORCED\ SAND}/E_{SAND}$ versus *Axial Strain in Triaxial Compression for Fabric Reinforced Dense and Loose Sand.*

deformations or strains in the sand which occur by this stage are small. At the beginning of the test, the normal stress is not high enough to force the geotextile to deform to the shape of the sand particles, and the developed contact efficiency value between geotextile and sand is small. The stiffness of the geotextile governs its ability to deform in the direction perpendicular to its plane; therefore, flexible geotextile provides a larger contact efficiency.

These results are consistent with the behavior of dense and loose sand whose angles of internal friction were 39° and 32° respectively. Haliburton and others [11] reported that the angle of sand–fabric friction for 5 different fabrics tested in special direct shear ranges from 37° to 46° for dense Mobile sand ($\phi_s = 50°$) and from 33° to 29° for the same sand in loose state ($\phi_s = 30°$).

Fabric Encapsulation Effect

Stress–deformation relationships for dense dune sand encapsulated in Geolon 400 and Geolon 200 are shown in Figure 9. As the sand compresses vertically

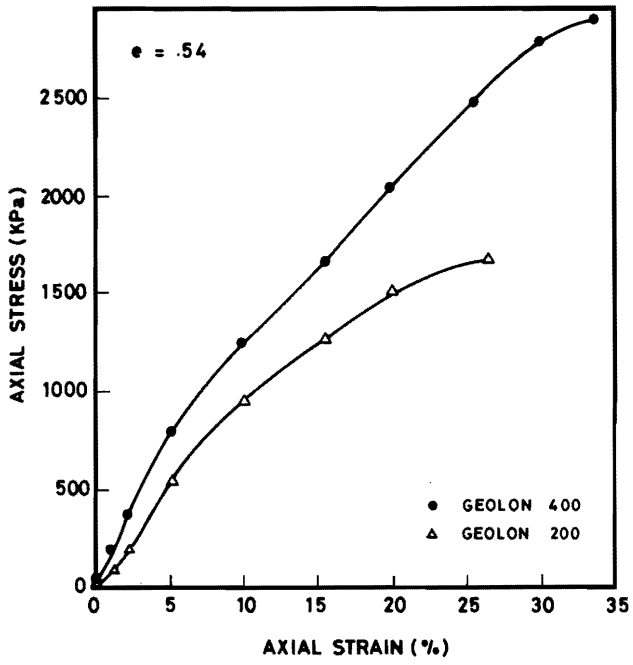

Figure 9. Stress–Deformation Relationships for Fabric Encapsulated Sand.

it also undergoes radial or lateral deformation. This lateral deformation causes fabric to stretch and develop a circumferential tensile stress (hoop stress). The magnitude of this hoop stress depends on the circumferential strain and modulus of the encapsulating fabric. The fabric hoop stress in turn exerts a radial confining stress on the encapsulated sand specimen which mobilizes its compressive strength and resistance to further deformation in an interactive or synergystic manner. From Figure 9 it can be observed that the stiffer Geolon 400 fabric induced a higher confining stress (or axial resisting stress) than that produced by Geolon 200. It should also be noted that large vertical strain (>25%) were required to mobilize the peak or maximum compressive stress in sand samples encapsulated in these relatively low modulus fabrics. In addition, the stress–deformation curve were non-linear with less and less compressive strength mobilized at successive increments of strains.

TESTS COMBINING ENCAPSULATION AND REINFORCEMENT

Influence of Combined Encapsulation Sand Reinforcement

The possible influence of three factors on the stress–deformation behavior were investigated, namely; (*a*) the ratio between the encapsulating and internal fabric modulus; (*b*) the fabric surface properties or interface friction characteristics; and (*c*) the tension stress–deformation properties of the internal reinforcement itself.

The presence of the internal reinforcement provides an additional quasi-confining stress, but it also simultaneously tends to reduce lateral deformation. The latter effect in turn compromises the effectiveness of the encapsulating fabric by reducing its hoop stress or confining stress.

The objective of using encapsulated/internally reinforced sand is not to maximize the effectiveness of one reinforcement system at the expense of another, but rather to improve the global properties of the reinforced composite body, *i.e.* to maximize its strength and/or minimize boundary deformations. Another objective is to avoid overstress in either reinforcement; this is particularly important in case of polymeric fabrics which are more vulnerable to creep and stress relaxation.

Figures 10 and 11 show the relationship between the deformation and axial stress for encapsulated

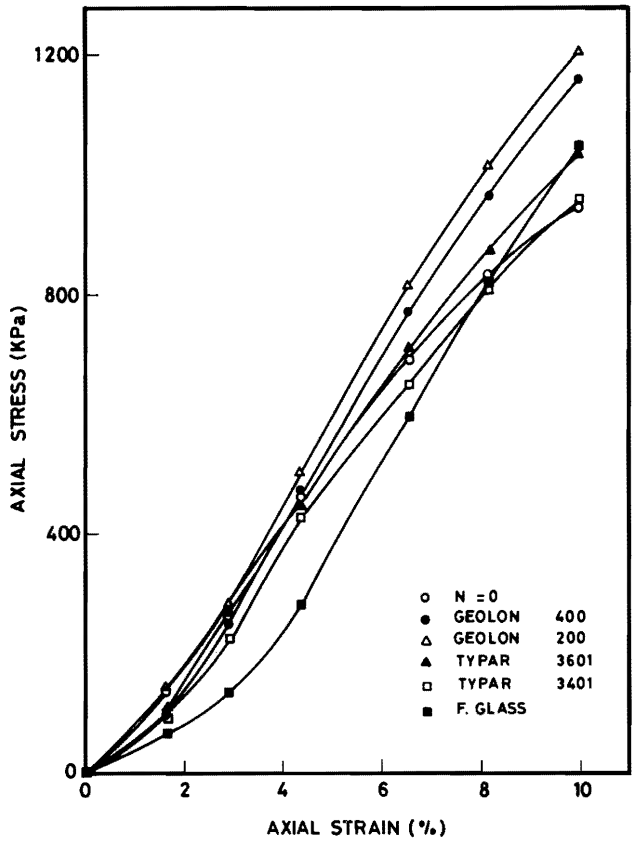

Figure 10. Stress–Deformation Relationship of Encapsulated Sand in Geolon 200 and Encapsulated Sand in Geolon 200/Internally Reinforced with Three Layers of Different Fabrics.

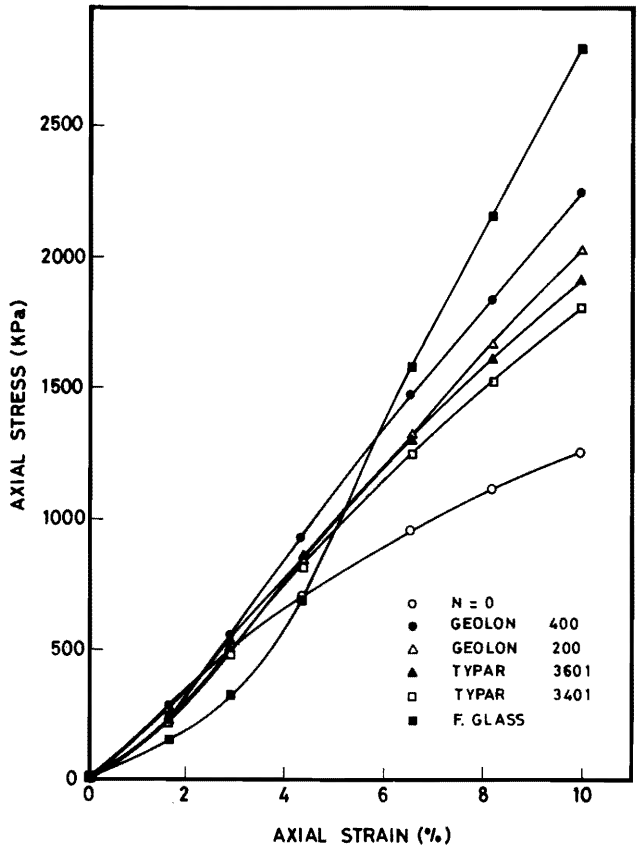

Figure 11. Stress–Deformation Relationship of Encapsulated Sand in Geolon 400 and Encapsulated Sand in Geolon 400/Internally Reinforced with Three Layers of Different Fabrics.

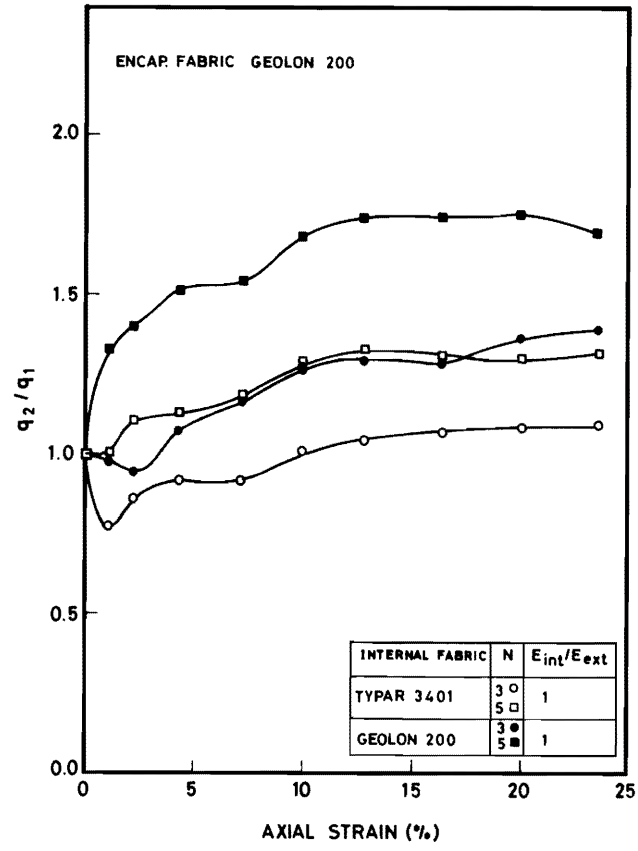

Figure 12. q_2/q_1 versus Axial Strain for Encapsulated/Internally Reinforced Sand with Geolon 200 and Typar 3401.

dense sand in Geolon 200 and Geolon 400 with and without internal reinforcements ($N=3$ and 5 layers). In both cases the internal reinforcement increased both the ultimate compressive strength and stiffness of the encapsulated sand except for stiff internal reinforcement (Fiberglass 196) which resulted in a loss of rigidity at low strain.

Influence of Internal Reinforcement Surface Properties

Figure 12 shows q_2/q_1 (uniaxial compressive strength for encapsulated sand/uniaxial compressive strength for encapsulated–internally reinforced sand) for sand encapsulated in Geolon 200 and internally reinforced with Geolon 200 and Typar 3401; they have the same modulus at 5% strain but the interface frictional properties are different. This figure indicates that the woven fabric, which has a larger interface friction, is more efficient in increasing the maximum axial stress and stiffness of the reinforced sand than the melt bonded nonwoven fabric, Typar 3401.

Influence of Modulus Ratio of Internal Fabric to External Fabric (E_{int}/E_{ext}) and Amount of Internal Reinforcement

Figure 13 shows the relationship between q_2/q_1 and E_{int}/E_{ext} at different strain levels. Figure 13 shows that the ratio between the secant modulus of the internal and the encapsulating fabrics (E_{int}/E_{ext}) should be a round unity in order to maximize the strength of encapsulated sand. Large (E_{int}/E_{ext}) ratio is effective only at high strain (>8%).

For sand encapsulated in "soft" fabric (Geolon 200) increasing the number of internal reinforcement layers increases the ratio of q_2/q_1 at any strain level.

For sand encapsulated in "rigid" fabric (Geolon 400) increasing the number of internal reinforcement layers increases the ratio of q_2/q_1, at high strain level (8%). At very low strain (<2%) increasing the internal reinforcement layers resulted in loss of stiffness.

Figure 14 shows the relationship between $(\varepsilon_{\bar{h}})_{max}/(\varepsilon_h)_{max}$ (where $(\varepsilon_{\bar{h}})_{max}$ = maximum horizontal strain

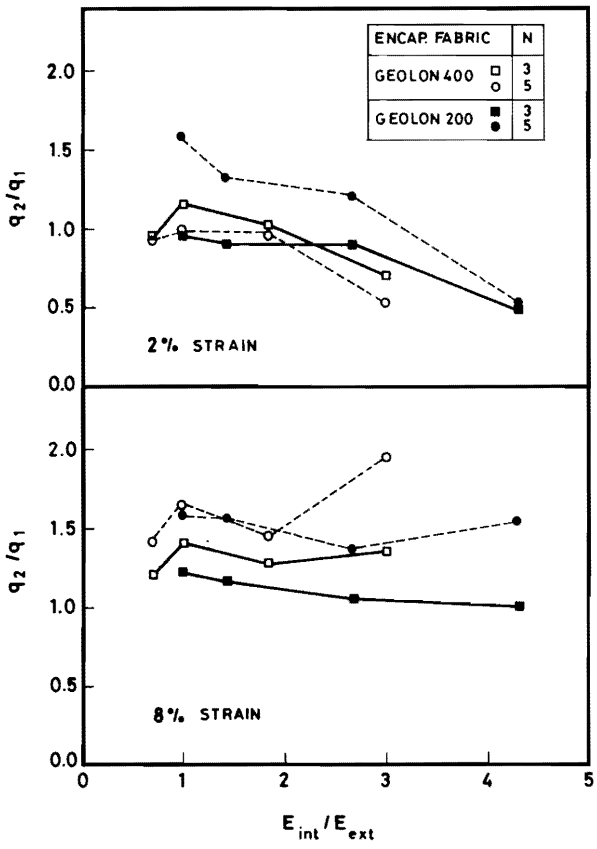

Figure 13. The Relationship Between q_2/q_1 Ratio and E_{int}/E_{ext} Ratio for Encapsulated/Internally Reinforced Sands.

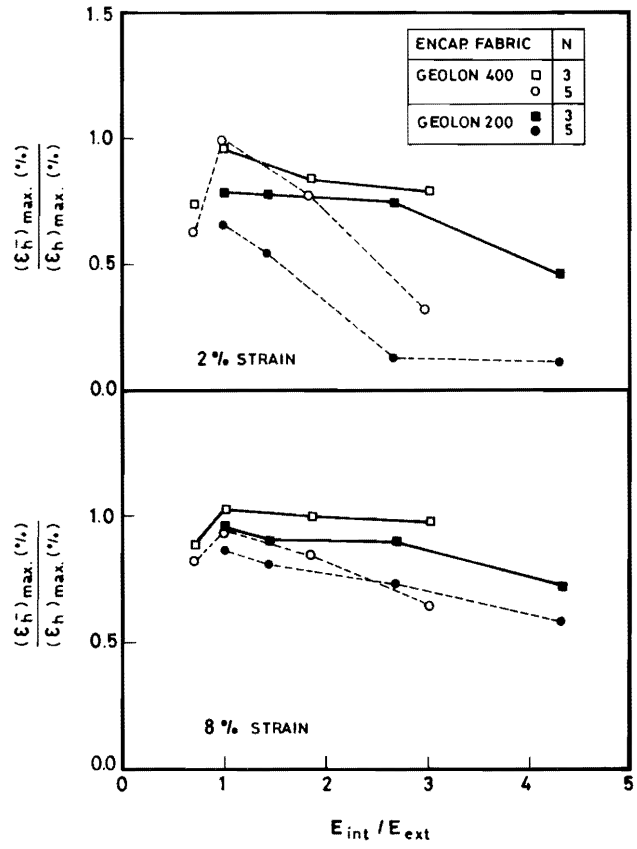

Figure 14. The Relationship Between $(\varepsilon_{\bar{h}})_{max}/(\varepsilon_h)_{max}$ Ratio and E_{int}/E_{ext} Ratio for Encapsulated/Internally Reinforced Sand.

of encapsulated sample at sample mid height and $(\varepsilon_h)_{max}$ = maximum horizontal strain of encapsulated/internally reinforced sample at sample mid height between two layers) and E_{int}/E_{ext} at different strain levels. Figure 14 shows that increasing the (E_{int}/E_{ext}) ratio effectively reduces the lateral deformation at low strain, whereas little or no reduction occurs in the lateral deformation at higher strain levels. If the objective is to maximize the strength and/or minimize boundary deformations the ratio between the secant modulus of internal and external fabric (E_{int}/E_{ext}) should be between 1–2.

Practical Applications

The paper indicates feasibility of using fabric reinforcement in granular columns or trenches beneath footing in order to increase bearing capacity and reduce settlement (increase stiffness).

Reinforcement is incorporated into granular columns or trenches as follows: fabric is placed at predetermined spacing in horizontal layers between successive lifts of sand. The sand or granular media is placed dry at maximum density by "air pluviation" or equivalent method.

The results indicate value of conjunctive fabric encapsulation around granular columns to provide additional confining stress $(\Delta\sigma_{3ext})$ where in-situ lateral stresses (mobilized passive resistance) may be inadequate, *viz.* at the top of column where lateral earth pressures are low, encapsulation can be achieved by:

placing prewoven fabric sleeve in bored hole (stiff soils) followed by backfilling;

forcing fabric sleeve into ground on a Mandrel which is withdrawn after backfilling (soft, squeezing soils).

CONCLUSIONS

1. Continuous, oriented fabric inclusions markedly increased the ultimate strength, increased the axial strain at failure; and limited reductions in post-peak shearing resistance.

2. At low strains (<1%) reinforcement produced a loss of stiffness with the effect being more pronounced the greater the number of layers and the stiffer the reinforcement.
3. Reinforcement placed at spacing/diameter ratio more than one had little effect on strength.
4. To maximize the strength and/or minimize boundary deformations of encapsulated/internally reinforced sand the ratio between the secant modulus of internal and external fabric (E_{int}/E_{ext}) should be between 1−2.
5. Increasing the amount of internal reinforcement increases the stiffness at any strain level of sand encapsulated in soft fabric and at high strain level of sand encapsulated in rigid fabric.

REFERENCES

[1] R. M. Koerner and J. P. Welsh, *Construction and Geotechnical Engineering Using Synthetic Fabrics.* New York: Wiley, 1980.
[2] J. R. Bell and R. G. Hicks, "Evaluation of Test Methods and Use Criteria for Geotechnical Fabrics in Highway Application", *Federal Highway Administration, Report No. FHWA/RD-80/021,* 1980.
[3] J. P. Giroud, "Geotextiles and Geomembranes", *Geotextiles and Geomembranes Journal,* **1(2)** (1984), p. 5.
[4] F. Schlosser and N. T. Long, "Behavior of Reinforced Earth for Retaining Structures", *Proceedings, 5th European Conference on Soil Mechanics and Foundation Engineering, Madrid,* vol. 1, 1972, p. 299.
[5] F. Schlosser and N. T. Long, "Recent Results in French Research on Reinforced Earth", *Journal of Construction, ASCE,* **100(3)** (1974), p. 223.
[6] Z. Yang, "Strength and Deformation Characteristics of Reinforced Sand", *Ph.D. Dissertation, University of California at Los Angeles,* 1972.
[7] M. R. Hausmann, "Strength of Reinforced Soil", *Proceedings, Australian Road Research Board,* **6** (1976), p. 1.
[8] J. K. Mitchell and F. Schlosser, "General Report", *Proceedings, International Conference on Soil Reinforcement, Reinforced Earth and Other Techniques, Paris,* vol. 1, 1979, p. 25.
[9] T. S. Ingold, *Reinforced Earth.* London: Thomas Telford Ltd, 1982.
[10] D. H. Gray, G. Athansopoulos, and H. Ohashi, "Internal/External Fabric Reinforcement of Sand", *Proceedings, 2nd International Conference on Geotextiles, Las Vegas,* vol. 3, 1982, p. 611.
[11] T. A. Haliburton, C. C. Anglin, and J. D. Lawmaster, "Selection of Geotechnical Fabrics for Embankment Reinforcement", *Contract No. DACWOL-78-C-0055 for U.S. Army Engineer District, Mobile, Alabama.* School of Civil Engineering, Oklahoma State University, Stillwater, 1978.

Paper Received 2 April 1988; Revised 14 September 1988.